Journal of Applied Physics

The optical and electrical properties of silver nanowire mesh films

Cite as: J. Appl. Phys. **114**, 024302 (2013); https://doi.org/10.1063/1.4812390
Submitted: 30 April 2013 • Accepted: 11 June 2013 • Published Online: 08 July 2013

G. Khanarian, J. Joo, X.-Q. Liu, et al.


View Online

Export Citation

CrossMark

ARTICLES YOU MAY BE INTERESTED IN

Electrical limit of silver nanowire electrodes: Direct measurement of the nanowire junction resistance
Applied Physics Letters **108**, 163302 (2016); https://doi.org/10.1063/1.4947285

Optical haze of randomly arranged silver nanowire transparent conductive films with wide range of nanowire diameters
AIP Advances **8**, 035201 (2018); https://doi.org/10.1063/1.5020033

New figure of merit for transparent conductors
Journal of Applied Physics **47**, 4086 (1976); https://doi.org/10.1063/1.323240

AIP Publishing

© 2013 AIP Publishing LLC.

The optical and electrical properties of silver nanowire mesh films

G. Khanarian,[1,a)] J. Joo,[2] X.-Q. Liu,[1] P. Eastman,[1] D. Werner,[1] K. O'Connell,[2] and P. Trefonas[2]
[1]*The Dow Chemical Company, 727 Norristown Rd., Spring House, Pennsylvania 19477, USA*
[2]*The Dow Chemical Company, 455 Forest St, Marlborough, Massachusetts 01752, USA*

(Received 30 April 2013; accepted 11 June 2013; published online 8 July 2013)

We present experimental results for the transmission T, haze H, sheet resistance R_s, and its spatial fluctuations ΔR_s for silver nanowire films. Mie light scattering theory of nanowires is developed to predict both T and H as a function of diameter D of wires and the surface fraction ϕ_s covered by the wires. Percolation theory is used to derive an equation for R_s in terms of D, the aspect ratio of wires D/L and ϕ_s. The critical exponent t for percolation of R_s is found to be 1.23 in close agreement with theoretical results for 2D random resistive networks ($t = 1.3$). These equations show the importance of both the distributions of diameter $\langle D \rangle$ and aspect ratio of wires $\langle D \rangle \langle L \rangle / \langle L^2 \rangle$ to predict the optical and electrical properties. Spatial fluctuations $\Delta R_s/R_s$ can also be significant in these films and be greater than 10% as ϕ_s approaches the critical percolation concentration ϕ_c. We show that the calculated T versus R_s and H versus R_s curves are in good agreement with the experimental data. We propose figures of merit for percolating nanowire films in terms of high T, low H, and low R_s to order the quality of films for touch screen applications. The results show that $D < 50$ nm and $L > 5$ μm are needed to achieve low haze $H < 1\%$, high transmission $T > 90\%$, together with low $R_s \sim 100$ Ω/sq for touch screen applications. Finally, we present experimental and theoretical results of the real and imaginary refractive indices of AgNW/polymer nanocomposites, and find that the Van De Hulst model is more accurate than the Maxwell Garnett models. © *2013 AIP Publishing LLC*. [http://dx.doi.org/10.1063/1.4812390]

I. INTRODUCTION

Silver nanowires (AgNW) have received a lot of attention recently as a potential replacement for Indium Tin Oxide (ITO) for transparent conductor (TC) applications.[1] They are attractive because they can be coated roll to roll from solution on large area flexible or rigid substrates, resulting in thin films with high optical transmission and low sheet resistance. Silver nanowires films are intrinsically different from ITO or thin metal films in so far that they are not continuous but consist of discrete nanowires that form a random resistive network.[2] The electrical properties can be understood in terms of percolating networks;[3] from this arises a number of unique features, namely, the critical percolation concentration ϕ_c below which there is loss of conductivity and the critical exponent of conductivity t. The critical exponent t for electrical conductivity has been studied by many theoreticians for 2D and 3D materials. A consequence of percolation is that sheet resistance and also its spatial fluctuations increases nonlinearly as the critical percolation concentration ϕ_c is approached. The optical properties of discrete nanowires are properly understood within the framework of Mie scattering theory which can predict both transmission T and scattering haze H. Scattering haze is particularly important in touch screens for display applications. It can reduce clarity and contrast especially when a display is viewed in the sunlight. Minimizing haze H is one of the key challenges when using nanowires in displays. On the other hand, for solar cell applications, one would like to maximize scattering to increase cell efficiency. The diameter D of the wire determines scattering and transmission, whereas the critical percolation concentration ϕ_c is also determined by the aspect ratio D/L of the nanowire, where L is its length. We also study the effect of a distribution of diameters $\langle D \rangle$ and lengths $\langle L \rangle$ on scattering and percolation. We show that two critical figures of merit (FOM) are transmission T versus sheet resistance R_s, and haze H versus R_s. A challenge is defining a figure of merit for nanowire coatings that is relatively independent of film thickness and nanowire concentration. The refractive index of nanocomposite films containing nanowires has also not been discussed widely in the literature and we present here both experimental results and theoretical calculations. The refractive index of nanowires films is important for designing anti reflection (AR) multilayer films. It is clear from this introduction that metal nanowire films have many interesting electrical and optical properties which are inherently different from continuous conductors such as ITO or thin metal films.

A. Electrical percolation of nanowires in 2D and 3D films

Metallic nanowires and carbon nanotubes have been synthesized and studied by many workers.[1(b)] Gruner and coworkers[2] used the percolation relation for sheet resistance

$$R_s \sim \frac{M}{(n_s - n_c)^t} \tag{1}$$

to determine the critical percolation concentration n_c (number of wires/area at percolation) and the critical exponent t,

[a)]Author to whom correspondence should be addressed. Electronic mail: gkhanarian@gmail.com.

 © 2013 AIP Publishing LLC

but did not determine the material constant M. Here, n_s is the number of wires per area. Subsequently, several workers[4–7] have used this equation to characterize t and n_c in terms of the diameter D and length L of nanowires. The early Monte Carlo work[8] deduced that $n_c = 18/\pi L^2$ but they assumed a uniform length L. Actual nanowire systems consist of a distribution of lengths $\langle L \rangle$ and diameters $\langle D \rangle$; $\langle n_c \rangle$ has been analyzed by a number of workers[9,9(k),10] theoretically and a number of relationships have been deduced in terms of the higher moments of L and D but with few experimental studies to support the predictions. Theoretical studies of random resistive networks have predicted that $t \sim 1.3$ for 2D networks and $t \sim 2$ for 3D networks,[3,11] but these studies assume that t is a constant and independent of L and D; experimental results presented here and Monte Carlo results by others suggest otherwise. Also, the experimental studies on silver nanowires and carbon nanotubes do not discuss spatial fluctuations in resistance, which are inherent in percolating films.[12] Analogous critical phenomena exhibit a nonlinear increase in fluctuations as criticality is approached.

B. Optical properties of nanowires based on Mie theory

The optical properties of nanowires have been modeled as thin continuous metallic films[5(c),5(g)] which clearly do not admit to scattering and haze; we show in this work that scattering is inherent to these systems and one must use a scattering model to calculate haze. Recently, Wiley *et al.* has modeled wires using finite difference time domain (FDTD) models,[7] but we show here that Mie scattering of nanowires is very accurate and more versatile to use than FDTD. Yet, another aspect of these films is the refractive indices $n_{composite}$ and $k_{composite}$ of polymer composites containing nanowires. This is important to calculate because silver nanowire films may be used together with antireflection coatings and one would need the optical constants to model multilayer films. The calculation of $n_{composite}$ and $k_{composite}$ is complicated by the well known depolarization of the local optical field due to the large aspect ratio of the metal nanowires. In summary, previous workers have discussed some of the aspects of the optical and electrical properties of metallic nanowires but have not presented a comprehensive explanation of the many phenomena such as scattering and haze, refractive index of nanocomposites, fluctuations in sheet resistance, and dependence on the distribution of diameters and lengths.

We present a more complete analysis of the optical and electrical properties of metal nanowires. We measured the optical transmission, haze, refractive index, average sheet resistance R_s, and its spatial fluctuations ΔR_s for several nanowire systems, as a function of concentration and spin coating speed on glass substrates. The data are analyzed with a model that we derive here. The starting point is the Mie theory of metal nanowires for optical transmission from which we deduce the fraction of area covered by silver nanowires ϕ_s. This parameter is analogues to the volume fraction in 3D materials. We then formulate a theory of haze, derived by Willmouth[13] for spheres and apply it to nanowire films. We also formulate the sheet resistance percolation equation in terms of ϕ_s and fit it to several experimental nanowire systems with different diameters D and length L and distributions. The Mie theory is an exact theory and has no fitting parameters, depending only on the diameter D and the optical constants n_m, k_m of silver. The percolation theory has three fitting parameters which give insight into the role of $\langle D \rangle$, $\langle L \rangle$ and its higher moments in determining n_c, t, and M in Eq. (1).

II. EXPERIMENTAL METHODS AND DATA ANALYSIS

The silver nanowires were obtained from commercial sources and are designated as suppliers 1–6. They were typically available as 1% w/w in water. They were formulated with a polymer binder with a refractive index $n_{polymer} = 1.51$ so that the weight fraction w of nanowire to polymer varied from about 20% to as high as 70%. Spin coating process was used to coat glass slides at various spin coating speeds 700–2000 rpm (Model P6700 Speciality Coating Systems, Indianapolis, IN) followed by drying of the films at 120 °C for 5 min. The thickness and surface roughness of some of the films were measured with a Veeco Dektak (Model 150) surface profilometer. The optical transmission was measured with a UV-VIS spectrometer (Hewlett Packard Lambda 9) and the total transmission (TT) and haze were measured with a Hunterlab Ultrascan XE or a BYK Haze gard meter. The films were also characterized with scanning electron microscopy (SEM) (JEOL 6700 FESEM) to determine the average diameter and lengths $\langle x \rangle$ and their respective root mean square (rms) deviations Δx. The experimental L and D were fitted to a lognormal distribution $f(x) = \frac{1}{x\sigma\sqrt{2\pi}} e^{-\frac{(\log x - \mu)^2}{2\sigma^2}}$, where $\mu = \log\langle x \rangle - 1/2 \log(1 + [\frac{\Delta x}{\langle x \rangle}]^2)$, $\sigma^2 = \log(1 + [\frac{\Delta x}{\langle x \rangle}]^2)$. The length and diameter of AgNW that we tested did not show noticeable correlation within SEM analysis. The distribution function f(x) was used to calculate averages $\langle D \rangle$, $\langle L \rangle$, and $\langle L^2 \rangle$. Table I lists the nanowires used in this study, their average diameters and lengths $\langle x \rangle$ and their respective rms deviations Δx.

III. MIE THEORY OF TRANSMISSION, HAZE, AND REFRACTIVE INDEX

A. Transmission with volume fraction of nanowires

The direct transmission of light T through a thickness d, consisting of n_v wires per volume, is given by

$$T = e^{-n_v C_{ext} d}, \tag{2}$$

where C_{ext} is the extinction coefficient of nanowires; n_v is related to volume fraction of rods ϕ_v, diameter D, and length L, by $n_v = \frac{\phi_v}{L\pi(\frac{D^2}{4})}$. The extinction coefficient at normal incidence is given by Mie[14]

TABLE I. Average diameters D and lengths L, their standard rms deviations ΔD, ΔL, respectively, measured by SEM, and calculated average extinction coefficients C_{ext}/wire volume, and scattering efficiency Q_{ext} (C_{ext}/wire area) for silver nanowires, $\lambda_0 = 600$ nm.

Nanowire	⟨D⟩ (nm)	ΔD (nm)	⟨L⟩ (μm)	ΔL (μm)	Q (⟨Cext⟩/wire area)	⟨Cext⟩/wire volume(μm^{-1})
S-1	100	23	36	16	1.59	19.2
S-2	70	16	16	16	1.12	19.47
S-3	56	9	8.6	4.1	0.814	18.1
S-4	71	17	7.6	3.5	1.14	19.27
S-5	132	28	14.8	10	1.83	16.9
S-6	153	42	4.8	4	1.91	14.76

$Q = 2\lambda/\pi\langle T_s(0) + T_p(0)\rangle/2\langle D\rangle$, $\langle Cext\rangle/\langle vol\rangle$ (μm^{-1}) $= 8\lambda/\pi^2\langle T_s(0) + T_p(0)\rangle/2\langle D^2\rangle$.

$$
\begin{aligned}
C_{ext,s} &= \frac{2\lambda L}{\pi} Re[T_s(0)] = Re\left[\frac{2\lambda L}{\pi}\left(a_0 + 2\sum_{n=1}^{\infty} a_n\right)\right],\\
C_{ext,p} &= \frac{2\lambda L}{\pi} Re[T_p(0)] = Re\left[\frac{2\lambda L}{\pi}\left(b_0 + 2\sum_{n=1}^{\infty} b_n\right)\right],\\
C_{ext} &= 1/2(C_{ext,p} + C_{ext,s}),\\
T_s(\theta) &= a_0 + 2\sum_{1}^{\infty} a_n \cos(n\theta),\\
T_p(\theta) &= b_0 + 2\sum_{1}^{\infty} b_n \cos(n\theta),
\end{aligned}
\tag{3}
$$

where L is the length of the nanowire and λ is the wavelength in medium, $\lambda = \lambda_0/n$, λ_0 and n being the wavelength in vacuum and refractive index of medium, respectively. $C_{ext,p,s}$ are the extinction coefficients for light incident at normal incidence polarized along and perpendicular directions of the nanowire. $T_s(\theta)$ and $T_p(\theta)$ are dimensionless quantities describing the angular dependence of scattering. By the Optical Theorem,[14] the extinction coefficient C_{ext} is related to T(0), i.e., scattering in the forward direction $\theta = 0$. The coefficients a_n and b_n are given by several authors;[14,15] they are a function of the diameter of the rods and their relative refractive indices to the surrounding medium, but not the length L. In the case of metallic nanowires, the refractive index is complex $n_m + ik_m$ and a function of wavelength. In randomly oriented wire networks which are usually encountered, one takes the average of T_s and T_p. Combining Eqs. (2) and (3), we arrive at the following equation relating direct transmission T to the optical parameters, the film thickness, and volume fraction of silver in the film

$$\log_e T = -d\phi_v \frac{8\lambda}{\pi^2} \frac{1/2[T_s(0) + T_p(0)]}{D^2}. \tag{4}$$

This equation relates the direct transmission T to the average extinction coefficient C_{ext}, diameter D, film thickness d, and volume fraction ϕ_v. The volume fraction is related to the weight fraction of silver nanowires in the film w by $\phi_v = \frac{w\alpha}{1-w(1-\alpha)}$, where α is the ratio of densities of polymer to silver, α = density(polymer)/density(silver) ∼ 1/10.5 ∼ 0.1.

B. Transmission with surface fraction of nanowires

We found from numerous studies that as the film thickness d became ∼100 nm or less and comparable to the diameter of the wires, then it became difficult to measure it accurately. Instead, we found that a better representation was to rewrite the transmission equation in terms of the number of wires/area n_s. Equation (2) is now written as

$$T = e^{-n_s C_{ext}}. \tag{5}$$

Note that in Eq. (5) the thickness d of the film does not appear directly. n_s is related to the surface area fraction ϕ_s by $n_s = \frac{\phi_s}{DL}$ and can be rewritten in terms of ϕ_s as

$$\log_e T = -\phi_s \frac{2\lambda}{\pi} \frac{1/2[T_s(0) + T_p(0)]}{D} = -\phi_s 1/2(Q_{ext,p} + Q_{ext,s}), \tag{6}$$

where ϕ_s is the fraction of surface area covered by AgNW. The advantage of this equation is that from a measurement of optical transmission T and the Mie calculation of the scattering extinction efficiency $Q = C_{ext}/DL$, one can estimate the surface faction ϕ_s. The surface fraction covered by AgNW is a more natural parameter to characterize very thin films, since the film thicknesses approach that of the diameter of the wires (50–100 nm), and electrical percolation in 2D films is also characterized by that parameter.

All the above equations can be extended to the case where there are a distribution of diameters and lengths. Since SEM analysis shows that D and L are uncorrelated, one finds that

$$
\begin{aligned}
-\mathrm{Log}\, T &= d\phi_v \frac{8\lambda}{\pi^2} \frac{1/2\int [T_s(0) + T_p(0)] f(D) dD}{\int D^2 f(D) dD}\\
&= d\phi_v \frac{8\lambda}{\pi^2} 1/2(\langle T_s(0)\rangle + \langle T_p(0)\rangle)/\langle D^2\rangle,
\end{aligned}
\tag{7}
$$

$$
\begin{aligned}
-\mathrm{Log}\, T &= \phi_s \frac{2\lambda}{\pi} \frac{1/2\int [T_s(0) + T_p(0)] f(D) dD}{\int D f(D) dD}\\
&= \phi_s \frac{2\lambda}{\pi} 1/2(\langle T_s(0)\rangle + \langle T_p(0)\rangle)/\langle D\rangle).
\end{aligned}
\tag{8}
$$

The above equations are equivalent, and so one deduces the relation between surface and volume fraction by

$$\phi_s = \frac{4}{\pi}\frac{\langle D\rangle}{\langle D^2\rangle}\phi_v d. \quad (9)$$

Note that when d ~ D, then $\phi_s \sim \phi_v$, but ϕ_s depends on both volume fraction and thickness of films.

To test the validity of Eq. (9), we made thicker films containing S-3 nanowires with measured thickness d and *w* fraction (hence known ϕ_v). We also measured the optical transmission T of the films to deduce ϕ_s from Eq. (8). Figure 1 is a plot of ϕ_s versus $\phi_v d$. The experimentally measured slope in Figure 1 is ~15, whereas the predicted slope according to Eq. (9) is 21.6, since $\langle D\rangle/\langle D^2\rangle \sim 17$ for the S3 wire. It is interesting to note that the experimental data show a linear dependence between ϕ_s and ϕ_v d as predicted by Eq. (9), but there is some discrepancy between the calculated and experimental slopes. Some of this discrepancy is caused by the fact that the log normal fit to the experimentally measured distribution of wire diameters is only approximate and so the estimate $\langle D\rangle/\langle D^2\rangle$ using the log normal fit may be inaccurate. Another cause of the discrepancy is the error made in thickness measurements. As we discussed above, there is considerable variations in film thickness due to the wires sticking out of the film. The use of optical transmission T to deduce ϕ_s is useful because it gives an average value over the entire film and we have found that it is possible to express both the Mie optical equations and percolation equations in terms of ϕ_s.

C. Optical transmission: Theory and experiment

Optical transmission measurements were carried out on thin films of AgNW mixed in a polymer matrix. Solutions were prepared by mixing AgNW in water, adding polymer binder, spin coating on a glass slide, and then baking at 120 °C for 5 min to dry the films. Optical transmission measurements were carried out with an UV VIS spectrometer. The glass background was subtracted to give essentially the transmission of the AgNW/polymer film. For each sample, we determined ϕ_s using Eq. (8). Figure 2 is a plot of transmission at $\lambda_0 = 600$ nm versus ϕ_s for the nanowires S1, S-3, and S-6 studied here which span the range of diameters D = 50–150 nm. Clearly, the slope is the extinction efficiency ⟨Q⟩ which is calculated from Mie theory and Eq. (3).

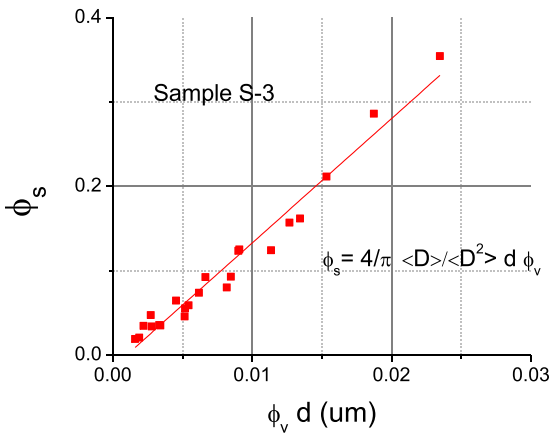

FIG. 1. Surface fraction ϕ_s as measured by optical transmission, versus $\phi_v d$ as measured by weight fraction of AgNW in film and its thickness d, for S-3 nanowire of Table I.

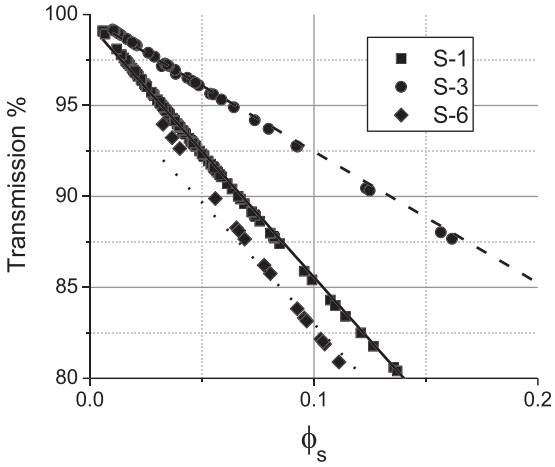

FIG. 2. Optical transmission versus silver area coverage ϕ_s for S-1, S-3, and S-6 nanowires.

Those are listed for the various nanowires in Table I. As expected, the slope is greater for the larger diameter wires.

We also measured the transmission as a function of wavelength for a number of films with different amounts of silver in them. The measured film thickness was d ~ 50 nm and the weight fraction of AgNW was w = 40%–50% w/w. The results are shown in Figure 3. Also shown are the calculations of transmission using Eq. (2). The calculation requires the n_m, k_m of silver, for which we have used the Drude model parameterization of Rakic *et al.*[16] We have also assumed that the refractive index of the binder is 1.51. We note that transmission off resonance decreases slightly with increasing silver. The plasmon resonance at 370 nm is due to confinement of light by the finite width of the nanowire. The agreement between experiment and theory is good, though there are some differences in the width of the transmission near resonance.

D. Haze from nanowires

Another unique property of AgNW based transparent conductors is the light scattering behavior. Haze was measured on each spin coated sample and we also determined the ϕ_s by the transmission method described above. Figure 4

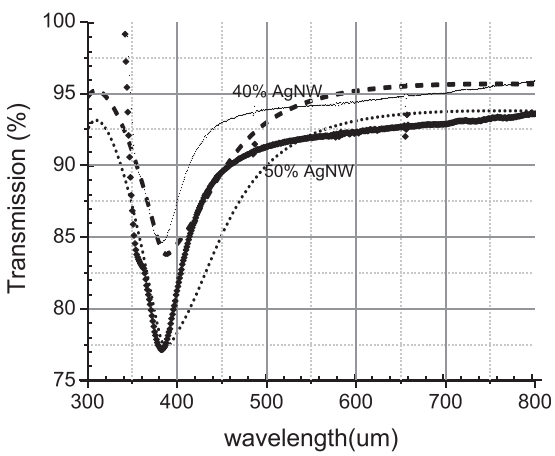

FIG. 3. Optical transmission versus wavelength for S-3 nanowire films with thickness d = 50 nm and w% = 40 (thin continuous line) and 50% loadings (thick continuous line). Calculated curves are shown as (- - - - -, 40% AgNW) and (……., 50% AgNW).

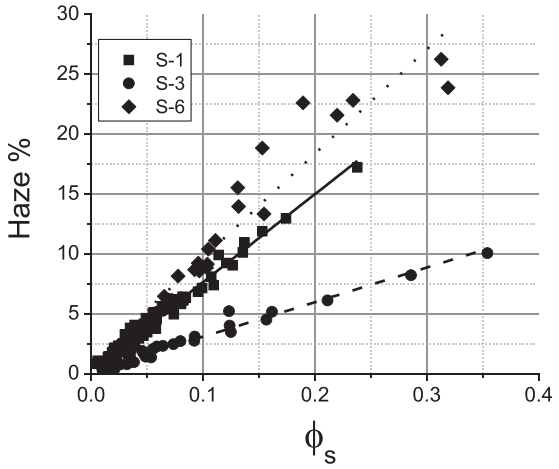

FIG. 4. Optical haze versus silver area coverage ϕ_s for nanowires S-1, S-3, and S-6. Calculated curves are shown as (_____, S-1), (- - - - - - - -, S-3) and (……, S-6).

shows the haze as a function of ϕ_s for the various wires studied here. One can see that haze appears to scale linearly with ϕ_s and increases significantly with diameter. We also show in Figure 4 the calculation of haze based on an equation that we have derived below—see Eq. (12). The agreement between experiment and theory is fairly good. For display applications, haze has to be kept to a minimum (usually <1%) and so one has to minimize either the amount of silver or thickness of the film. However, for photovoltaic applications, one would like to maximize haze from electrodes to increase optical path length in the cell.

In order to derive an expression for haze, we extend the derivation of Willmouth[13] for haze from spheres to nanowires. The reader should consult Ref. 13 for the derivation for spheres. We present here the final results for scattering from nanowires. Consider the scattering geometry depicted in Figure 5, and see Appendix for detailed derivation.

Light is incident on a substrate and then travels and is scattered in a thin film containing AgNW. We assume that we can approximate the Fresnel transmission[17] terms by the average values $F_{ij} = \frac{4n_i n_j}{(n_i+n_j)^2}$ at each optical interface and that thin film resonant effects are negligible. That approximation

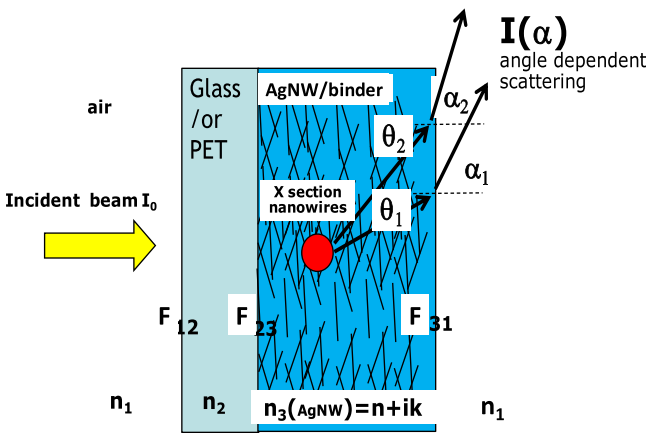

FIG. 5. Scattering geometry of nanowires in films.

is valid because we observe very small ripple effects when we measure T versus wavelength. The light is scattered with internal angle θ and exits the film at angle α. They are related to each other by Snell's law. The scattering efficiency between angles θ_1 and θ_2 is given by

$$\langle C_{\alpha 1}^{\alpha 2}\rangle = \frac{2\lambda L}{\pi}\int_0^\infty f(D)dD\int_{\theta 1}^{\theta 2} 1/2(F_{s31}|T_s(\theta)|^2 + F_{p31}|T_p(\theta)|^2)\sin\theta d\theta, \quad (10)$$

where $F_{s,p}$ are the angular dependent Fresnel transmission factors[13,17] for the two polarizations s,p,

$$F_{s31}(\theta) = \frac{\sin(2\theta)\sin(2\alpha)}{\sin^2(\theta+\alpha)}, \quad F_{p31}(\theta) = \frac{\sin(2\theta)\sin(2\alpha)}{\sin^2(\theta+\alpha)\cos^2(\theta-\alpha)}. \quad (11)$$

Haze is the scattered radiation outside the main beam. According to ASTM D1003 standard testing protocol, the scattered light is measured from 2.5° to 90°, and is normalized by the total transmission, and not the incident flux. The expression for haze for nanowires becomes (see Appendix)

$$H = \frac{F_{12}F_{23}\frac{\langle C_{2.5}^{90}\rangle}{\langle C_{ext}\rangle}(1-e^{-\phi_s\langle Q_{ext}\rangle})}{F_{12}F_{23}F_{31}e^{-\phi_s\langle Q_{ext}\rangle} + F_{12}F_{23}\frac{\langle C_0^{90}\rangle}{\langle C_{ext}\rangle}(1-e^{-\phi_s\langle Q_{ext}\rangle})}. \quad (12)$$

We calculate $H(\%)/\phi_s$ as a function of diameter $\langle D\rangle$ at the off resonance wavelength $\lambda = 600$ nm and compare it with experimental results obtained from Figure 4, i.e., the slopes of the straight lines in Figure 4 and the results are shown in Figure 6. Since ϕ_s is low for AgNW based percolated transparent conductor, we assume no multiple scattering among nanowires and no overlap effects. However, these assumptions need to be adjusted for high ϕ_s condition. The agreement between theory and experiment is fairly good.

It shows that haze is a strong function of the diameter in the range D = 0–200 nm. For example, at D = 50 nm, $H(\%)/\phi_s$ is ~30%. Therefore, if the display requires 1% haze then $\phi_s \sim 0.03$ or less. This sets an upper bound on the amount silver/unit area. If instead D = 100 nm, then $H(\%)/\phi_s$ is

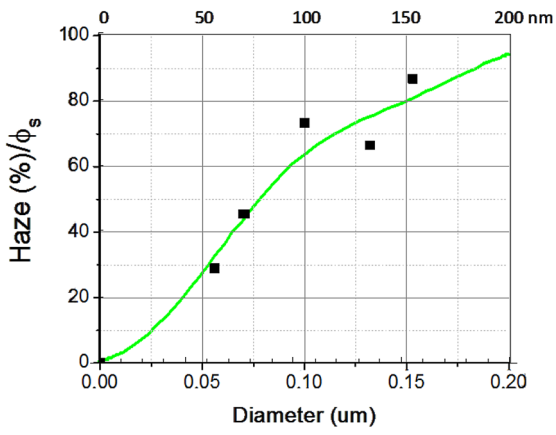

FIG. 6. Slope of Haze(%) versus ϕ_s, Haze(%)/ϕ_s, as a function of AgNW diameter.

TABLE II. Best fit parameters to Eq. (18). Column 1 is the designated and its average diameter. Column 2 is the calculated value of $\langle L\rangle\langle D\rangle/\langle L^2\rangle$ based on the lognormal fit to the experimental D and L SEM data. Columns 3-5 are the best fits parameters of Eq. (18) to the sheet resistance R_s versus ϕ_s data. $1/M'$ is the material parameter, ϕ_c is the critical percolation concentration and t is the critical exponent for percolation.

Nanowires (diameter nm)	$\langle L\rangle\langle D\rangle/\langle L^2\rangle$	Prefactor $1/M'$	Critical percolation concentration ϕ_c	Critical exponent t
S-1(100)	0.004	1.26	0.03	1.19
S-2 (70)	0.00254	0.77	0.016	1.24
S-3(56)	0.0053	0.36	0.0165	1.06
S-4(71)	0.0077	0.32	0.043	1.18
S-5(132)	0.0073	1.17	0.022	1.08
S-6(153)	0.0215	~1.5	0.11	1.01

~60%, and so if the display requires H ~ 1%, then $\phi_s \sim 0.017$ or less. It is interesting to compare these requirements on ϕ_s with those obtained from electrical percolation theory and measurements, discussed later in this paper. Percolation theory stipulates that ϕ_s must be greater than ϕ_c, where ϕ_c is the critical percolation concentration. Table II above reports the experimental values of ϕ_c for the different wires obtained from sheet resistance measurements. One finds that when D = 100 nm (S-1 nanowire), then $\phi_c \sim 0.03$ which is greater than $\phi_s \sim 0.017$ required to achieve H < 1%. Therefore, we conclude that a nanowire with diameter D = 100 nm cannot satisfy the haze requirement of H < 1%. On the other hand, for a nanowires with diameter D ~ 50 nm (S-3), $\phi_c \sim 0.0165$ which is less than the required $\phi_s = 0.03$ to achieve H < 1%. Therefore, we conclude that nanowires with D ~ 50 nm should be able to satisfy the H < 1% requirement for display applications.

E. Refractive index of nanowires

The refractive index of spherical metal particles in polymer nanocomposites has been studied widely[18] especially within the scope of the Maxwell Garnett (MG) and Brugemann mean field approximations, but nanowires have received less attention. We measured the refractive index of thin films containing 20 and 30% w/w% of S-2/polymer film spin coated on silicon wafers, with a spectroscopic Woollam α SE ellipsometer. The data were analyzed with a B-Spline method[19] and are shown in Figures 7 and 8 for the real $n_{composite}$ and imaginary $k_{composite}$ values versus wavelength, respectively. We tested two models for the calculation of the refractive index, the MG model[18] and another one due to Van de Hulst.[14(a)]

1. Maxwell Garnett equation

The Maxwell Garnett equation[18] for the complex optical dielectric constant $\varepsilon_{composite}$ of a nanocomposite consisting of randomly oriented rod assembly is given by

$$(1-\phi_v)\frac{(\varepsilon_{composite}-\epsilon_{polymer})}{(\varepsilon_m-\varepsilon_{composite})} = \frac{\phi_v}{3}\sum_{i=1}^{3}\frac{\epsilon_{polymer}}{\epsilon_{polymer}+L_i(\varepsilon_m-\varepsilon_{polymer})}, \quad (13)$$

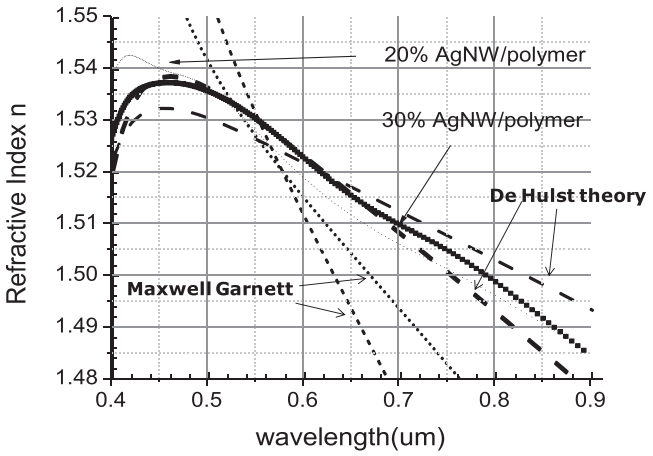

FIG. 7. Real refractive index n of 20, 30% w/w S-2 AgNW/polymer composite. Experimental measurements are thin and thick continuous lines for 20% and 30% AgNW/polymer, respectively. Theoretical calculations are by the theories of Van De Hulst (– – – – – –, thick, thin) and Maxwell Garnett (……, thick, thin) for 20 and 30% AgNW/polymer, respectively.

where L_i are the depolarization factors and are tabulated by Van De Hulst, Meeten, and Bohren for various shapes.[14,20] For a long cylinder, $L_1 = 0$, $L_2 = L_3 = 1/2$ and ϕ_v is the volume fraction of nanowires. The various optical dielectric constants are defined below

$$\epsilon_m = \epsilon'_m + i\epsilon''_m, \quad \epsilon'_m = n_m^2 - k_m^2, \quad \epsilon''_m = 2n_m k_m, \quad (14)$$

where n_m and k_m are the real and imaginary refractive indices of Ag metal, respectively. They are given by the Drude model[14(b)] for Ag metal, parameterized by Rakic *et al.*[16] $\varepsilon_{polymer}$ corresponds to $n^2_{polymer}$, where $n_{polymer}$ is the refractive index of polymer.

2. Van De Hulst equation

The Van De Hulst equation derivation is based on Mie theory and it was studied and verified experimentally by Meeten for dilute latexes and rods.[20,21] Using rather general arguments, Van de Hulst derived (see also Bohren[14(b)] and Barrera[22]) the equation for real $n_{composite}$ and imaginary $k_{composite}$ refractive index of large objects in a dilute system. The dilute condition applies to the cases studied in this work since w = 30%–50% is equivalent to $\phi_v \sim 0.03$–0.05. The resulting equations are,

$$n_{composite} = n_{polymer}\left(1+\frac{2\pi n_v}{k^3}\frac{2L}{\lambda}\mathrm{Im}[1/2<T_s(0)+T_p(0)>]\right), \quad (15a)$$

$$k_{composite} = n_{polymer}\frac{2\pi n_v}{k^3}\frac{2L}{\lambda}\mathrm{Re}[1/2<T_s(0)+T_p(0)>], \quad (15b)$$

where $k = 2\pi/\lambda$. n_v is the number of rods/unit volume. Figure 7 shows the experimental real refractive index data for 20 and 30% w/w AgNW/polymer and also the theoretical calculations according to the two models. We assumed that refractive index of the polymer was 1.51.

Figure 8 shows the imaginary refractive index of the nanocomposite for 20 and 30% w/w in polymer, and the theoretical calculations according the MG and Van De Hulst models. The agreement between experimental and theory is excellent. We note that the experimental data for real $n_{composite}$ exhibit a maximum at 450 nm and a minimum in imaginary $k_{composite}$ near 600 nm. The Van de Hulst model can predict both the maximum and minimum and also the magnitude of $n_{composite}$ and $k_{composite}$. The MG theory fails to predict the wavelength dependence and also the magnitude of $n_{composite}$ and $k_{composite}$.

IV. PERCOLATION EQUATION FOR NANOWIRES FILMS

A. Sheet resistance of 2D periodic grid

We have demonstrated that the Mie theory gives an accurate prediction of the transmission, haze, and refractive index of AgNW/polymer nanocomposites as a function of ϕ_s and ϕ_v, respectively. The next step is to derive an equation for sheet resistance R_s in terms of ϕ_s, based on a random resistive network and Eq. (1). In order to help derive a complete equation including the material parameters such as resistivity ρ, diameter D, and length L of the nanowires, we first derive a simple equation for a *periodic* 2 D resistive network in terms of surface fraction covered by silver ϕ_s. Consider a square array of wires of diameter width D and periodicity L. The light transmission is $T = \frac{(L-D)^2}{L^2} = (1-\frac{D}{L})^2$. The amount of silver covering the surface is related to the amount of light which is blocked by the silver, $\phi_s = 1 - T = 1 - (1-\frac{D}{L})^2 \cong \frac{2D}{L}$, since usually D/L $\ll$ 1. Now, we derive the sheet resistance of such a 2D square periodic network. Let R be the resistance between each node on the grid. Then, it can be shown that the average sheet resistance R_s over a macroscopic distances (as measured by 4 point probe instrument) is also equal to R,[23] i.e., $R_s = R$. Now, the resistance R between two nodes is given by ρL/(wire cross sectional area), where ρ is the resistivity of silver, L is the length between nodes, divided by the cross sectional area of the wire of diameter D. Therefore, the sheet resistance of a periodic grid becomes $R_s = R = \frac{4\rho L}{\pi D^2}$. This can be expressed in terms of ϕ_s and D by

$$R_s = \frac{C8\rho}{\pi D\phi_s}. \tag{16}$$

Note that we have also replaced ρ by Cρ, C > 1, because the resistivity is sometimes greater than pure metal due to processing and junction resistances. Equation (16) relates the sheet resistance of a periodic 2D square array of wires to the diameter D and the fraction of the surface covered by metal. Both larger diameter and larger ϕ_s will lower sheet resistance. Note that for a continuous metal thin film of thickness D, then $R_s = \rho/D$. The $8/\pi$ factor in Eq. (16) is a geometrical factor arising from the circular cross section of the wire, which reduces the effective metal content relative to a continuous metal film, and so raises the sheet resistance.

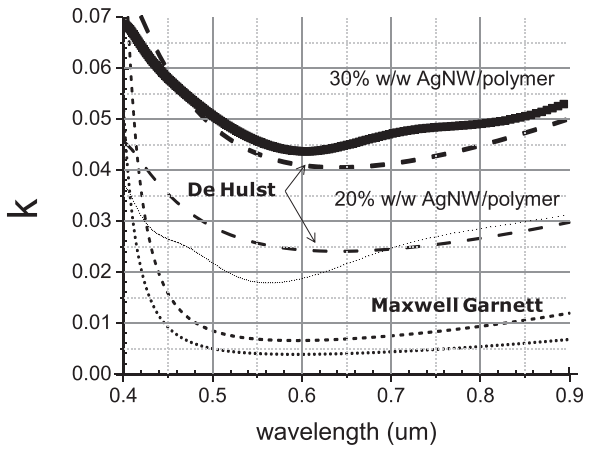

FIG. 8. Imaginary refractive index k of 20, 30% w/w S-2 AgNW/polymer composite. Experimental measurements are thin and thick continuous lines for 20% and 30% AgNW/polymer, respectively. Theoretical calculations are by the theories of Van De Hulst (– – – – –, thick, thin) and Maxwell Garnett (……, thick, thin) for 20% and 30% AgNW/polymer, respectively.

B. Estimate of material constant for random resistive percolating network

A periodic 2D array of wires does not exhibit critical behavior as ϕ_s decreases, in contrast to random resistive percolating nanowires (see Eq. (1)). However, in the latter system, as the silver concentration increases above the critical percolation concentration ϕ_c, one would expect that a percolating wire network to behave more and more like a regular wire network and eventually a continuous metallic film. We now rewrite Eq. (1) in terms of ϕ_s and ϕ_c to make this analogy clearer. Since the area of a wire is DL, it follows that $n_s = \phi_s/DL$ and $n_c = \phi_c/DL$. Now, Monte Carlo simulations and geometrical arguments show that $n_c = 18/\pi L^2$. Therefore, $\phi_c = 18D/\pi L$. Equation (1) can now be rewritten as

$$R_s \sim \frac{M'}{(\phi_s - \phi_c)^t}. \tag{17}$$

This equation analogous to a similar 3D percolating wire equation that is written in terms of volume fraction ϕ_v and used by others.[6(a)] In Eq. (17), when $\phi_s \gg \phi_c$, then $R_s \sim \frac{M'}{(\phi_s)^t}$, where t $\sim$ 1.3 for a 2D film. Previously, we derived for a 2D *periodic* network of wires $R_s = \frac{C8\rho}{\pi D\phi_s}$, where the exponent for ϕ_s in the denominator was 1. By comparing the two equations, we hypothesize that $M' = \frac{C8\rho}{\pi D}$ is the approximate material constant. Experimental results show that this is not an unreasonable approximation. However, this is an area of research that could be studied further to help elucidate the material factor M′ more rigorously.

C. Effect of distribution of diameter and length on critical percolation concentration

Another aspect of percolating networks that have received little attention is the role of the distribution of nanowire diameters ⟨D⟩ and lengths ⟨L⟩. Many workers[9(a),9(d),9(g)] have pointed that the critical percolation concentration, n_c, can be derived by using geometric arguments of adjoining

areas A_c touching one another, swept out by nanowire length L; thus $A_c n_c \sim 1$, where $A_c \sim \pi L^2/4^2$. Note the exact result is $A_c = \pi L^2/18$. If one has a distribution of lengths, then similar geometric arguments would yield the following result $n_c \sim 4^2/\pi\langle L^2\rangle$ as long as the distribution was not too wide. Similarly, the cross sectional area of a nanowire would be $\langle DL\rangle \sim \langle D\rangle\langle L\rangle$ since we find from SEM analysis that diameters and lengths of nanowires are generally not correlated. Combining the above results, one arrives at the following for the critical area fraction, $\phi_c = 18\langle D\rangle\langle L\rangle/\pi\langle L^2\rangle$. Thus, the percolation Eq. (17) becomes

$$R_s = \frac{\frac{8}{\pi}\frac{\rho}{D}C}{\left(\phi_s - \frac{18}{\pi}\frac{\langle D\rangle\langle L\rangle}{\langle L^2\rangle}\right)^t}. \tag{18}$$

D. Determination of fit parameters for percolation equation

On each sample that was prepared for transmission and haze measurements, we also carried out sheet resistance measurements using the four point probe method.[24] A Jandel four point probe instrument was used to measure the sheet resistance many times across the film and we calculated its average value and its root mean square deviation from the mean. Thus, we recorded for each film the T, from which we deduce the ϕ_s, the haze H, the sheet resistance R_s, and its rms fluctuation ΔR_s. We observed that ΔR_s increased with R_s as the concentration approached the critical concentration ϕ_c. Thus, when $R_s > 200$ Ω/sq, the fluctuations became significant (>10%). Figure 9 is a plot of R_s versus ϕ_s for the nanowires.

It is noted in Figure 9 that the R_s appears to increase nonlinearly as ϕ_s approaches different values of ϕ_c dictated by the different values of $\phi_c = 18\langle D\rangle\langle L\rangle/\pi\langle L^2\rangle$, see Table II for those values for different nanowires. In order to facilitate the analysis of the data, we plotted $1/R_s$ versus ϕ_s, since there is more scatter and error in measuring high sheet resistance values R_s. We used the following procedure to facilitate the fitting of Eq. (18) to the experimental data. We plot $\frac{1}{R_s} = (\frac{1}{M'})(\phi_s - \phi_c)^t$, where $\frac{1}{M'} = \pi D/8\rho C$, $\phi_c = \kappa\langle D\rangle\langle L\rangle/\langle L^2\rangle$, and C, κ, and t are fitting parameters. Figure 10 is a plot of $1/R_s$ vs ϕ_s for the various wires S-1, S-3, and S-6 listed in Table I. Note the almost linear dependence of $1/R_s$ versus the silver coverage ϕ_s.

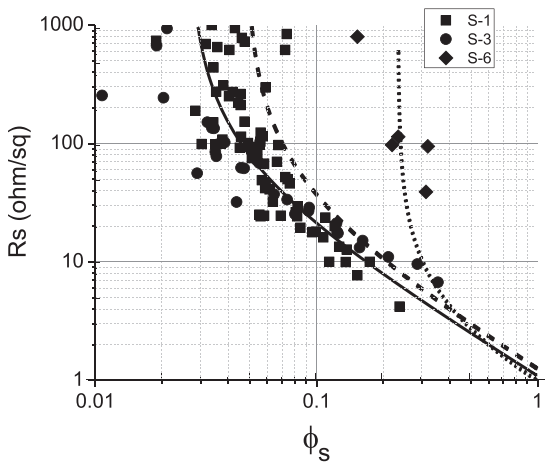

FIG. 9. Sheet resistance R_s versus silver area coverage ϕ_s for S-1, S-3, and S-6 nanowires. The sheet resistance increases nonlinearly as the critical percolation concentration ϕ_c is approached. It is different for every wire and is a function of $\langle L\rangle\langle D\rangle/\langle L^2\rangle$.

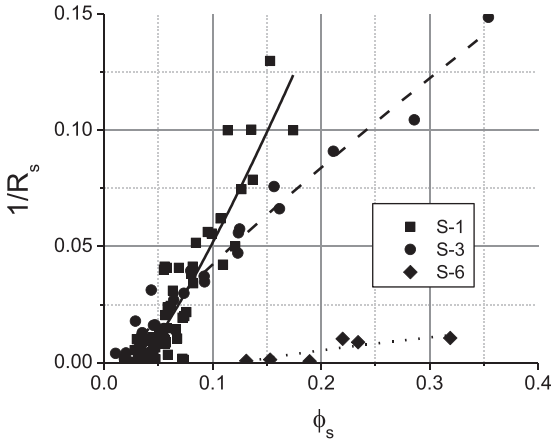

FIG. 10. $1/R_s$ versus ϕ_s for S-1, S-3, and S-6, nanowires. The curves are the best fits to the data with the equation $\frac{1}{R_s} = \left(\frac{1}{M'}\right)(\phi_s - \phi_c)^t$. (_____, S-1), (- - - - - -, S-3), and (……., S-6).

In Table II, we give the best fit parameters 1/M′, ϕ_c, and t to the experimental data for all the nanowires listed in Table I. We have also calculated $\langle D\rangle\langle L\rangle/\langle L^2\rangle$ using the experimental SEM data in Table I and assuming the lognormal fit to the standard deviation in diameter and length.

We want to understand the dependence of the fit parameters on the nanowires dimensions. The fitting parameters 1/M′ is plotted versus the diameter D in Figure 11. We equate the best fit slope 10.1 to $\pi/(8\rho$ C). Since $\rho = 0.016$ Ω μm for silver, then we deduce that C = 2.4. If C = 1, then the wires would have metallic conductivity. The fact that C ~ 2.4 implies that the wires have greater resistivity than pure silver metal, probably because of the junction resistance between the wires.

We plot the critical percolation concentration ϕ_c versus $\langle D\rangle\langle L\rangle/\langle L^2\rangle$ in Figure 12. The slope is found to be 5.67

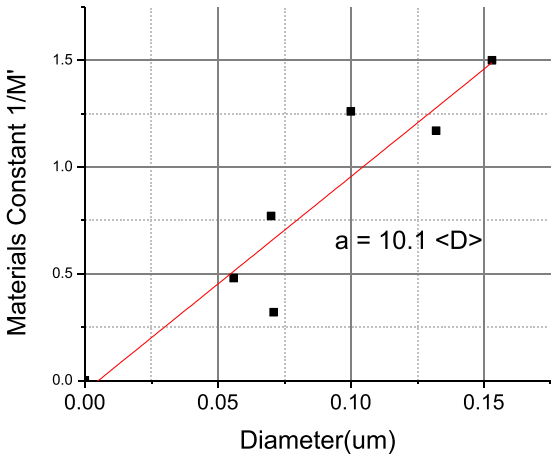

FIG. 11. Material parameter 1/M′ versus nanowire diameter $\langle D\rangle$.

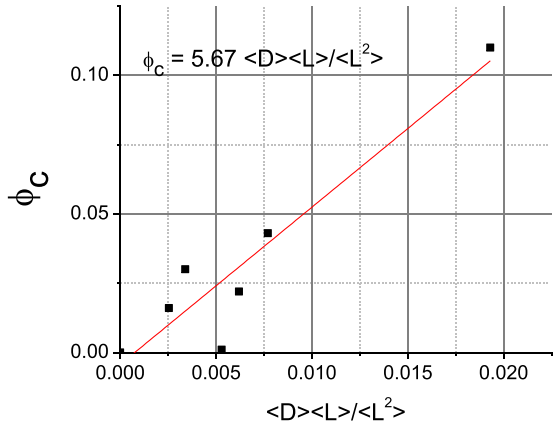

FIG. 12. Critical percolation concentration ϕ_c versus nanowire aspect ratio $\langle D\rangle\langle L\rangle/\langle L^2\rangle$, calculated in Table II.

which is close to the theoretical value $18/\pi = 5.73$. ϕ_c is the most critical parameter that determines the dependence of R_s versus ϕ_s, and determines indirectly other relationships such as T vs R_s and H versus R_s.

Finally, we plot the critical exponent t versus $\langle D\rangle\langle L\rangle/\langle L^2\rangle$ in Figure 13. We find that as the aspect ratio $\langle D\rangle\langle L\rangle/\langle L^2\rangle$ approaches zero, the critical exponent approaches 1.23. The theoretical prediction for a 2D percolating network is $t = 1.3$.[11,25] We observe a small dependence of the critical percolation exponent on the aspect ratio. Foygel *et al.*[26] found in their simulations that t decreased with aspect ratio of rods L/D; however, our results suggest that t decreases with D/L. Further work must be done to understand the dependence of critical exponent t with aspect ratio.

Thus, we conclude that the simple percolation model presented here accounts for most of the observed features and the experimental fits are close to the theoretical predictions. Note that the parameters that have been derived are the average for six different AgNW systems. However, each one varies somewhat from the norm. The sheet resistance data for the various nanowires show a number of interesting features that are worth noting. The most unique aspect is that R_s increases nonlinearly as the silver coverage ϕ_s approaches ϕ_c, which is very distinctive of percolating systems. Also, ϕ_c varies for different nanowires because it is dependent on the aspect ratio D/L. Finally to obtain low R_s values as required for various transparent conductor applications, the AgNW coverage ϕ_s-ϕ_c must attain a certain minimum value, i.e., one cannot lower AgNW concentration and make the films arbitrarily sparse and still expect to obtain low Rs. This conflicts with the requirement that ϕ_s must be kept as low as possible in order to maximize T and minimize H for display applications. Therefore, one has to study the relation between T and R_s and also H and R_s to arrive at the optimal concentration of silver ϕ_s required to meet the design specifications for a transparent conductor.

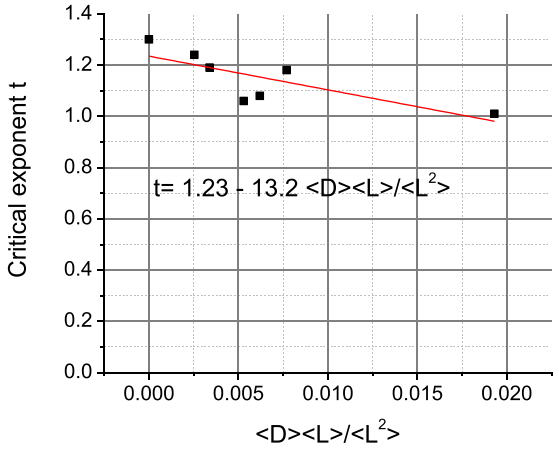

FIG. 13. Critical exponent t versus nanowires aspect ratio $\langle D\rangle\langle L\rangle/\langle L^2\rangle$, calculated in Table II.

V. TRANSMISSION AND HAZE VERSUS SHEET RESISTANCE: THEORY AND EXPERIMENT

We now present experimental plots of transmission and haze versus sheet resistance for the nanowires studied here, and compare them with theoretical predictions based on Eqs. (8), (12), and (18) for the transmission, haze, and sheet resistance. Figure 14 shows the transmission versus sheet resistance for the wires studied here, and the theoretical predictions for those nanowires based on the model presented here. Note that the calculated lines are not best fits to data, but the predictions of the model based on the Mie and percolation theories presented here. The results show that lower diameters generally give higher transmission at a given sheet resistance R_s. It is possible to achieve $T > 90\%$ when $R_s \sim 100\ \Omega$/sq when the diameters $D < 100$ nm.

Figure 15 shows the haze versus sheet resistance for the wires studied in this work and the predictions based on the model. These curves are not best fits but determined by the Mie theories of Eqs. (8), (12), and percolation equation (18). We find good agreement between the experimental and theoretical models. The results show that it is possible for H $\sim$ 1%–2%, $R_s \sim 100\ \Omega$/sq when the diameter D $\sim$ 50 nm or less. Haze is much more sensitive to diameter than transmission. Another aspect that should be noted is that the model calculations are somewhat sensitive to the value assumed for the critical percolation concentration ϕ_c. The reason for this uncertainty comes from the inaccuracy of measurements of

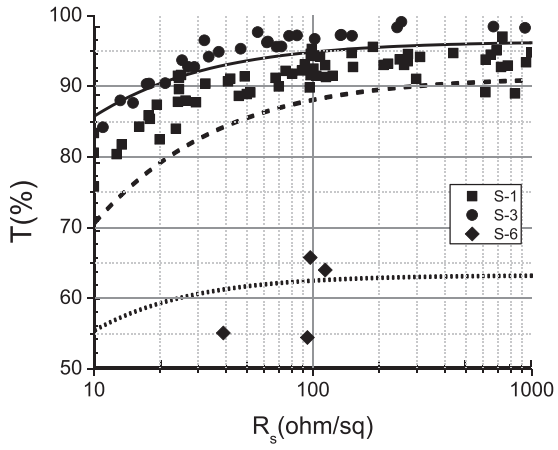

FIG. 14. Optical transmission versus sheet resistance R_s for S-1, S-3, and S-6 nanowires. Theoretical curves are (- - - - - - - -, S-1), (_____, S-3), and (……., S-6).

high sheet resistance values R_s because of fluctuations as the films become sparse. The effect of random fluctuations will be discussed further in Sec. VI.

The results of Figures 14 and 15 are interesting in that they show a number of trends. It is possible to obtain high transmission $T > 90\%$ with a low $R_s \sim 100\ \Omega$/sq if the wires have small enough diameters $D < 100$ nm. However, the T rolls off at lower Rs values and it is difficult to obtain high T at Rs $\sim 10\ \Omega$/sq unless the wires have very small diameters. The Haze H is even more sensitive to diameter than T as shown in Figure 15. Haze versus R_s also shows a tradeoff between low haze and high R_s, i.e., low silver content, but the result is highly dependent on diameter of the wires. This is because haze is directly caused by scattering from nanowires. To approach $H = 1\%$, one would need wires with diameter $D < 50$ nm at 100 Ω/sq. Haze increases rapidly with diameter as noted in Figure 6. It seems that even though larger diameter D will lower R_s, it is not enough to compensate for the increase in haze.

VI. SPATIAL FLUCTUATIONS IN SHEET RESISTANCE

We also observed significant fluctuations in sheet resistance ΔRs, when repeated measurements were done across the film surface, as shown in Figure 16. We note that the fluctuations measured can become significant (>10%) as the silver coverage decreases and approaches the critical percolation ϕ_c. We have drawn lines to indicate these trends; for example, S-6 has the largest fluctuations and S-3 has the smallest fluctuations. These are not best fits based on any models but merely to guide the reader to trends in the data. Fluctuations in sheet resistance are mainly due to two causes. First, fluctuation in local concentration of nanowires is inherent to percolating films. One observes in a SEM micrograph areas of open space without AgNW coverage, and these areas become larger as criticality is approached. Therefore, the four point probe will sample areas of different wire densities. Second, another source of fluctuations of R_s is due to film thickness variations. Both effects are incorporated in fluctuations $\Delta\phi_s$.

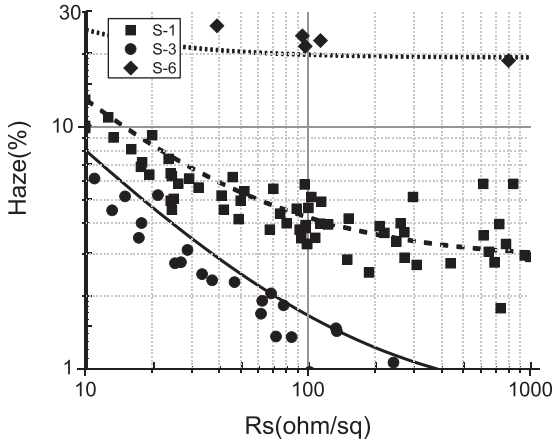

FIG. 15. Haze versus sheet resistance R_s, for S-1, S-3, and S-6 nanowires. Theoretical curves are (- - - - - -, S-1), (_____, S-3), and (……., S-6).

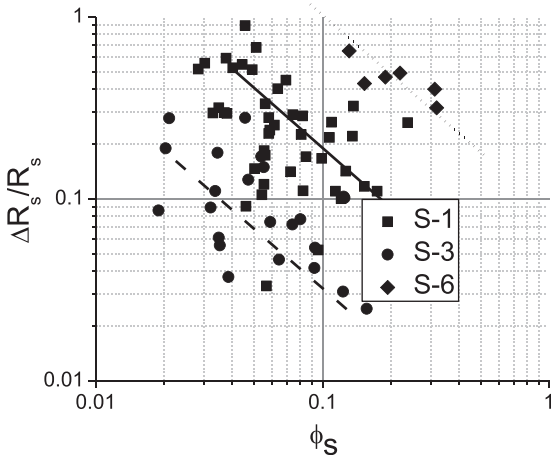

FIG. 16. Fluctuation in sheet resistance ΔRs/Rs versus silver surface coverage ϕ_s. Lines are drawn to guide reader to trends and are not best fit lines. (_____, S-1), (- - - - - - - -, S-3), and (……., S-6). Note the nonlinear increase in fluctuations as ϕ_s approaches the critical percolation concentration ϕ_c as described by Eq. (19).

We can attempt to arrive at a semi empirical equation for ΔRs by differentiating Eq. (18) with respect to ϕ_s to obtain

$$\frac{\sqrt{\langle \Delta R_s^2 \rangle}}{R_s} = \frac{t\sqrt{\langle \Delta \phi_s^2 \rangle}}{(\phi_s - \phi_c)}. \tag{19}$$

The above equation indicates that relative fluctuations in ΔRs are a function of the relative fluctuation in silver coverage $\Delta\phi_s$ and describe the broad features of the data of Figure 16, namely that fluctuations increase as ϕ_s approaches the critical concentration ϕ_c. Further investigation of these effects is needed to fundamentally understand the origin of these fluctuations; this is also important from a practical technological point of view, since fluctuations in sheet resistance may impact design of devices such as touch screens. As discussed earlier, the fluctuations ΔRs/Rs that one observes can be quiet large (>10%) when ϕ_s-$\phi_c \sim 0.05$ or less, which means that one cannot make films arbitrarily sparse for some practical applications. This may have technological implications in the use of nanowires in touch screens because the design engineers may specify the maximum fluctuations in R_s that their designs will allow. In turn, this will dictate the value of ϕ_s chosen, which in turn will determine sheet resistance, transmission, and haze.

VII. FIGURES OF MERIT FOR NANOWIRES FILMS

Finally, we discuss the issue of figure of merit (FOM) for films containing nanowires. Haacke[27] proposed a FOM for TCs as T^{10}/Rs, for materials such as ITO. In continuous TC, one only has to be concerned with the thickness of the film and one tries to find a FOM which is relatively independent of thickness. In the case of nanowires, there is the additional parameter of the concentration of nanowires in the film. Ideally, one would like a figure of merit that is relatively independent of concentration and thickness which

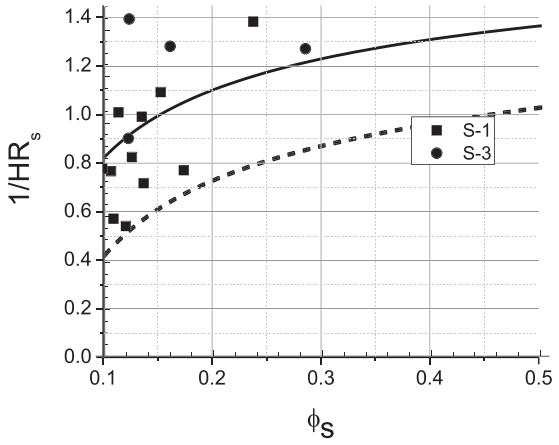

FIG. 17. Experimental FOM $1/HR_s$ versus silver area coverage ϕ_s for nanowires S-1 and S-3. Theoretical curves are (_____, S-1) and (- - - - - - -, S-3).

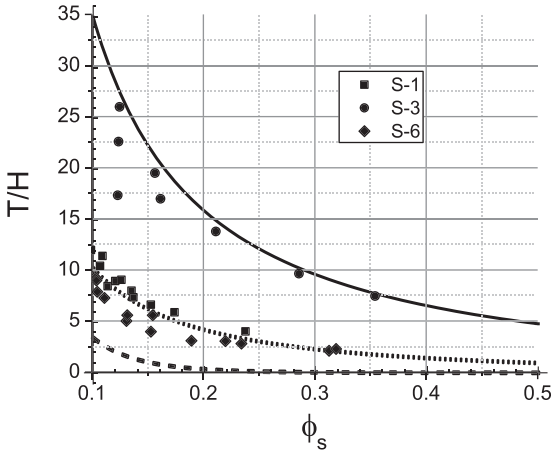

FIG. 19. Experimental T/H versus silver coverage ϕ_s for nanowires S-1, S-3, and S-6. Theoretical curves are (- - - - - -, S-1), (_____, S-3), and (……., S-6).

gives high transmission and low sheet Rs, i.e., T^{10}/Rs. Another feature of nanowires is that they exhibit light scattering and haze and one would like a FOM that measures low haze and low sheet resistance, i.e., 1/HRs. Finally, another possible figure of merit is high transmission and low H, i.e., T/H. In this section, we explore these three figures of merit as a function of AgNW coverage ϕ_s.

A. Low haze and sheet resistance, $1/(HR_s)$

Figure 17 gives the calculated $1/HR_s$ vs ϕ_s for two nanowires studied and the corresponding experimental results. One can see that the lower diameter sample give the highest FOM. The experimental points are in approximate accord with the theoretical curves computed according to the theory presented. It is somewhat difficult to define a FOM that is completely independent of ϕ_s, but it becomes less dependent at higher loadings.

B. High transmission and low sheet resistance, T^{10}/R_s

Figure 18 plots T^{10}/Rs for the three nanowires studied here. Again one finds approximate agreement between theory and experiment. Between $\phi_s = 0.1$–0.2, the curves are ordered approximately according to their diameter, i.e., S-3 has the highest FOM and S-6 has the lowest FOM. However, the plots of Figure 18 show that it is difficult to define a FOM which is independent of silver content.

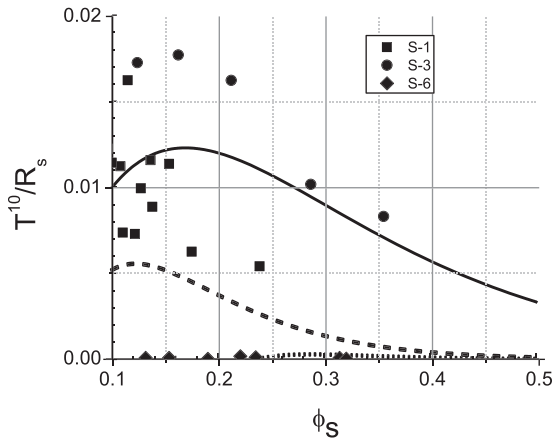

FIG. 18. Experimental FOM T^{10}/R_s versus silver coverage ϕ_s for nanowires S-1, S-3, and S-6. Theoretical curves are (- - - - - -, S-1), (_____, S-3), and (……, S-6).

C. High transmission and low haze, T/H

We also define a FOM independent of R_s, i.e., T/H which indicates the quality of film having high transmission and low haze. Figure 19 shows T/H for the nanowires studied here. One see that T/H could also be used as FOM to order the quality of AgNW. The agreement between theory and experiment is fairly good because the theory is based solely on Mie theory and does not involve the electrical percolation theory. However, this FOM is not as sensitive to differences between wires, i.e., it says that S-1 and S-6 are nearly equivalent whereas the FOM 1/HRs and T^{10}/Rs shows clear differences between these wires. Also, this FOM is more dependent on the concentration of wires, than the other FOMs. Therefore, all three FOM should be used with care to rank the quality of wires with respect to transmission, haze, and sheet resistance.

VIII. CONCLUSIONS

In conclusion, we have presented an analysis of the optical and electrical properties of silver nanowires based on Mie light scattering and electrical percolation theory. The Mie theory was used to calculate both the transmission and haze. Haze has not been previously discussed in detail by other authors. We used the surface area fraction covered with silver ϕ_s as a key parameter to formulate the theoretical expressions for T and H. We also developed a semi empirical expression for the sheet resistance R_s based on percolation theory. We analyzed experimental plots of T, H, and R_s versus ϕ_s and showed that theory agreed fairly well with experimental data. The sheet resistance increases nonlinearly as ϕ_s approaches the critical percolation concentration ϕ_c. The diameter D is the most important factor that determines haze and transmission, whereas the electrical properties are dependent on both diameter D, and also very sensitively on ϕ_c,

which is a function of $\langle D\rangle\langle L\rangle/\langle L^2\rangle$. The experimentally measured critical exponent t for percolation was very close to the theoretical predicted value of a 2D film. We also presented experimental results on the fluctuations of ΔRs, explained its origin qualitatively, and derived an approximate expression which is in accord with the experimental data. Spatial fluctuation can be significant (>10%) as ϕ_s approaches ϕ_c. We presented figures of merit for nanowires in terms of high T, low H, and low R_s to characterize nanowires mesh films for touch screen applications, and showed that these figures of merit are concentration dependent. We conclude that it is possible to make transparent conductors with high transmission T > 90% and low haze H∼ 1% with sheet resistance Rs ∼ 100 Ω/sq as long as the diameters D ∼ 50 nm or less, and the aspect ratio of the wires D/L ∼ 250 or greater. Finally, we presented experimental and theoretical results of the real and imaginary refractive indices of AgNW/polymer nanocomposites, and find that the Van De Hulst model is more accurate than the Maxwell Garnett models.

ACKNOWLEDGMENTS

We thank A. Malek, G. Athens, J. Lunn, T. Calverley, and M. de Graaf of The Dow Chemical Company for many stimulating discussions.

APPENDIX: DERIVATION OF HAZE EQUATION

We derive here the expression for haze from nanowires (Eq. (12)) following the derivation of Willmouth[13] for an assembly of spheres in a medium. Haze is defined as the transmitted diffuse light scattered from 2.5° to 90° $DT_{2.5}^{90}$ divided by the Total Transmission (TT)

$$H = \frac{DT_{2.5}^{90}}{TT}. \tag{A1}$$

The TT is defined as the direct transmission T(direct) plus the diffuse transmission DT_0^{90} from 0° to 90°

$$TT = T(direct) + DT_0^{90}. \tag{A2}$$

We derive expressions for the various terms in Eqs. (A1), (A2) by referring to Figure 5. The direct transmission is simply given by

$$T(direct) = F_{12}F_{23}F_{31}e^{-n_sC_{ext}}, \tag{A3}$$

where we have assumed no background subtraction and F_{ij} are the Fresnel transmission terms between the ith and jth layers.

We derive an expression for the diffuse transmission scattered between angles α_1 and α_2 in Figure 5, which is need to compute the haze. Consider a wire (shown in red) in Figure 5 at a distance x into the nanowire film. The flux of energy at a distance x is

$$T(x) = F_{12}F_{23}e^{-n_vC_{ext}x}. \tag{A4}$$

Let the fraction of energy scattered between angles α_1 and α_2 be given by $C_{\alpha 1}^{\alpha 2}$. Integration of $C_{\alpha 1}^{\alpha 2}$ over all angles gives the extinction coefficient C_{ext}. Since there are n_v rods/volume, then in an area A and thickness dx, the total number of rods is n_v Adx. The total energy scattered from this infinitesimal volume is given by

$$T_{\alpha 1}^{\alpha 2}(x) = F_{12}F_{23}e^{-n_vC_{ext}x}n_vC_{\alpha 1}^{\alpha 2}dx. \tag{A5}$$

Integrating over a thickness d, one obtains the total energy scattered between angles α_1 and α_2

$$T_{\alpha 1}^{\alpha 2}(d) = F_{12}F_{23}n_vC_{\alpha 1}^{\alpha 2}\int_0^d e^{-n_vC_{ext}x}dx. \tag{A6}$$

The resultant integration is

$$\begin{aligned} T_{\alpha 1}^{\alpha 2}(d) &= F_{12}F_{23}\frac{C_{\alpha 1}^{\alpha 2}}{C_{ext}}(1 - e^{-n_vC_{ext}d}) \\ &= F_{12}F_{23}\frac{C_{\alpha 1}^{\alpha 2}}{C_{ext}}(1 - e^{-n_sC_{ext}}). \end{aligned} \tag{A7}$$

The interpretation of Eq. (A7) is as follows. The light flux entering the nanowire film is $F_{12}F_{23}$ and the light flux exiting the film is $F_{12}F_{23}\exp(-n_vC_{ext}\,d)$. The difference is the total amount of light scattered, of which $\frac{C_{\alpha 1}^{\alpha 2}}{C_{ext}}$ is scattered between angles α_1 and α_2.

Next, we state an expression for $C_{\alpha 1}^{\alpha 2}$ in terms of the Mie scattering coefficients and the angular Fresnel transmission factors F_{s31} and F_{p31} (see Eq. (11) above for the definition)

$$C_{\alpha 1,rod}^{\alpha 2} = \frac{2\lambda L}{\pi}\int_{\theta 1}^{\theta 2} 1/2(F_{s31}|T_s(\theta)|^2 + F_{p31}|T_p(\theta)|^2)\sin\theta\; d\,\theta, \tag{A8}$$

where the integration is between the internal angles θ_1 and θ_2 which are related to the external angles by Snell's law. For the case of forward diffuse scattering, $\alpha_1 = 0$ and $\alpha_2 = 90°$ in Eq. (A2). For haze measurements, $\alpha_1 = 2.5$ and $\alpha_2 = 90°$ in the numerator term in Eq. (A1)

The expression for TT now becomes from Eqs. (A2), (A3), and (A7)

$$TT = F_{12}F_{23}F_{31}e^{-n_sC_{ext}} + F_{12}F_{23}\frac{C_0^{90}}{C_{ext}}(1 - e^{-n_sC_{ext}}). \tag{A9}$$

The expression for haze H becomes from Eqs. (A1), (A7), and (A9)

$$H = \frac{F_{12}F_{23}\frac{C_{2.5}^{90}}{C_{ext}}(1 - e^{-n_sC_{ext}})}{F_{12}F_{23}F_{31}e^{-n_sC_{ext}} + F_{12}F_{23}\frac{C_0^{90}}{C_{ext}}(1 - e^{-n_sC_{ext}})}. \tag{A10}$$

It is straightforward to show that for a distribution of diameters the haze becomes Eq. (12)

$$H = \frac{F_{12}F_{23}\frac{\langle C_{2.5}^{90}\rangle}{\langle C_{ext}\rangle}(1 - e^{-\phi_s\langle Q_{ext}\rangle})}{F_{12}F_{23}F_{31}e^{-\phi_s\langle Q_{ext}\rangle} + F_{12}F_{23}\frac{\langle C_0^{90}\rangle}{\langle C_{ext}\rangle}(1 - e^{-\phi_s\langle Q_{ext}\rangle})}, \tag{A11}$$

where the averages are over the diameter distribution (Eq. (10)) and $n_s C_{ext}$ is replaced by the average of the extinction efficiency $\phi_s \langle Q_{ext} \rangle$.

[1](a) D. S. Hecht and R. B. Kaner, "Solution-processed transparent electrodes," MRS Bull. **36**(10), 749–755 (2011); (b) Y. G. Sun, Y. D. Yin, B. T. Mayers, T. Herricks, and Y. N. Xia, "Uniform silver nanowires synthesis by reducing $AgNO_3$ with ethylene glycol in the presence of seeds and poly(vinyl pyrrolidone)," Chem. Mater. **14**(11), 4736–4745 (2002); (c) B. Wiley, Y. G. Sun, B. Mayers, and Y. N. Xia, "Shape-controlled synthesis of metal nanostructures: The case of silver," Chem.-Eur. J. **11**(2), 454–463 (2005); (d) Y. G. Sun and Y. N. Xia, "Large-scale synthesis of uniform silver nanowires through a soft, self-seeding, polyol process," Adv. Mater. **14**(11), 833–837 (2002).

[2]L. B. Hu, D. S. Hecht, and G. Gruner, "Carbon nanotube thin films: Fabrication, properties, and applications," Chem. Rev. **110**(10), 5790–5844 (2010).

[3]D. Stauffer and A. Aharony, *Introduction to Percolation Theory* (CRC Press, 1994).

[4](a) L. B. Hu, H. S. Kim, J. Y. Lee, P. Peumans, and Y. Cui, "Scalable coating and properties of transparent, flexible, silver nanowire electrodes," ACS Nano **4**(5), 2955–2963 (2010); (b) J. Y. Lee, S. T. Connor, Y. Cui, and P. Peumans, "Semitransparent organic photovoltaic cells with laminated top electrode," Nano Lett. **10**(4), 1276–1279 (2010); (c) W. Gaynor, J. Y. Lee, and P. Peumans, "Fully solution-processed inverted polymer solar cells with laminated nanowire electrodes," ACS Nano **4**(1), 30–34 (2010); (d) W. Gaynor, G. F. Burkhard, M. D. McGehee, and P. Peumans, "Smooth nanowire/polymer composite transparent electrodes," Adv. Mater. **23**(26), 2905 (2011); (e) B. E. Hardin, W. Gaynor, I. K. Ding, S. B. Rim, P. Peumans, and M. D. McGehee, "Laminating solution-processed silver nanowire mesh electrodes onto solid-state dye-sensitized solar cells," Org. Electron. **12**(6), 875–879 (2011).

[5](a) S. De, T. M. Higgins, P. E. Lyons, E. M. Doherty, P. N. Nirmalraj, W. J. Blau, J. J. Boland, and J. N. Coleman, "Silver nanowire networks as flexible, transparent, conducting films: Extremely high DC to optical conductivity ratios," ACS Nano **3**(7), 1767–1774 (2009); (b) L. F. C. Pereira, C. G. Rocha, A. Latge, J. N. Coleman, and M. S. Ferreira, "Upper bound for the conductivity of nanotube networks," Appl. Phys. Lett. **95**(12), 123106 (2009); (c) S. De, P. J. King, P. E. Lyons, U. Khan, and J. N. Coleman, "Size effects and the problem with percolation in nanostructured transparent conductors," ACS Nano **4**(12), 7064–7072 (2010); (d) F. S. F. Morgenstern, D. Kabra, S. Massip, T. J. K. Brenner, P. E. Lyons, J. N. Coleman, and R. H. Friend, "Ag-nanowire films coated with ZnO nanoparticles as a transparent electrode for solar cells," Appl. Phys. Lett. **99**(18), 183307 (2011); (e) V. Scardaci, R. Coull, P. E. Lyons, D. Rickard, and J. N. Coleman, "Spray deposition of highly transparent, low-resistance networks of silver nanowires over large areas," Small **7**(18), 2621–2628 (2011); (f) P. E. Lyons, S. De, J. Elias, M. Schamel, L. Philippe, A. T. Bellew, J. J. Boand, and J. N. Coleman, "High-performance transparent conductors from networks of gold nanowires," J. Phys. Chem. Lett. **2**(24), 3058–3062 (2011); (g) S. De and J. N. Coleman, "The effects of percolation in nanostructured transparent conductors," MRS Bull. **36**(10), 774–781 (2011); (h) S. Sorel, P. E. Lyons, S. De, J. C. Dickerson, and J. N. Coleman, "The dependence of the optoelectrical properties of silver nanowire networks on nanowire length and diameter," Nanotechnology **23**(18), 185201 (2012); (i) P. N. Nirmalraj, A. T. Bellew, A. P. Bell, J. A. Fairfield, E. K. McCarthy, C. O'Kelly, L. F. C. Pereira, S. Sorel, D. Morosan, J. N. Coleman, M. S. Ferreira, and J. J. Boland, "Manipulating connectivity and electrical conductivity in metallic nanowire networks," Nano Lett. **12**(11), 5966–5971 (2012).

[6](a) S. I. White, R. M. Mutiso, P. M. Vora, D. Jahnke, S. Hsu, J. M. Kikkawa, J. Li, J. E. Fischer, and K. I. Winey, "Electrical percolation behavior in silver nanowire-polystyrene composites: Simulation and experiment," Adv. Funct. Mater. **20**(16), 2709–2716 (2010); (b) R. M. Mutiso, M. C. Sherrott, J. Li, and K. I. Winey, "Simulations and generalized model of the effect of filler size dispersity on electrical percolation in rod networks," Phys. Rev. B **86**(21), 214306 (2012).

[7]S. M. Bergin, Y. H. Chen, A. R. Rathmell, P. Charbonneau, Z. Y. Li, and B. J. Wiley, "The effect of nanowire length and diameter on the properties of transparent, conducting nanowire films," Nanoscale **4**(6), 1996–2004 (2012).

[8](a) G. E. Pike and C. H. Seager, "Percolation and conductivity: A computer study. I," Phys. Rev. B **10**(4), 1421 (1974); (b) C. H. Seager and G. E. Pike, "Percolation and conductivity: A computer study. II," *ibid.* **10**(4), 1435 (1974).

[9](a) I. Balberg and S. Bozowski, "Percolation in a composite of random stick-like conducting particles," Solid State Commun. **44**(4), 551–554 (1982); (b) I. Balberg and N. Binenbaum, "Computer study of the percolation threshold in a two-dimensional anisotropic system of conducting sticks," Phys. Rev. B **28**(7), 3799 (1983); (c) I. Balberg, N. Binenbaum, and C. H. Anderson, "Critical behavior of the two-dimensional sticks system," Phys. Rev. Lett. **51**(18), 1605–1608 (1983); (d) I. Balberg, C. H. Anderson, S. Alexander, and N. Wagner, "Excluded volume and its relation to the onset of percolation," Phys. Rev. B **30**(7), 3933 (1984); (e) I. Balberg, N. Binenbaum, and N. Wagner, "Percolation thresholds in the three-dimensional sticks system," Phys. Rev. Lett. **52**(17), 1465–1468 (1984); (f) I. Balberg, "Universal percolation-threshold limits in the continuum," Phys. Rev. B **31**(6), 4053 (1985); (g) I. Balberg, "Excluded-volume explanation of Archie's law," *ibid.* **33**(5), 3618 (1986); (h) I. Balberg and N. Binenbaum, "Invariant properties of the percolation thresholds in the soft-core–hard-core transition," Phys. Rev. A **35**(12), 5174 (1987); (i) Z. Rubin, S. A. Sunshine, M. B. Heaney, I. Bloom, and I. Balberg, "Critical behavior of the electrical transport properties in a tunneling-percolation system," Phys. Rev. B **59**(19), 12196 (1999); (j) C. Chiteme, D. S. McLachlan, and I. Balberg, "1/f or flicker noise in cellular percolation systems," *ibid.* **67**(2), 024207 (2003); (k) L. Berhan and A. M. Sastry, "Modeling percolation in high-aspect-ratio fiber systems. I. Soft-core versus hard-core models," Phys. Rev. E **75**(4), 041120 (2007).

[10](a) S. Kumar, M. A. Alam, and J. Y. Murthy, "Computational model for transport in nanotube-based composites with applications to flexible electronics," ASME Trans. J. Heat Transfer **129**(4), 500–508 (2007); (b) Q. Cao, H. S. Kim, N. Pimparkar, J. P. Kulkarni, C. J. Wang, M. Shim, K. Roy, M. A. Alam, and J. A. Rogers, "Medium-scale carbon nanotube thin-film integrated circuits on flexible plastic substrates," Nature **454**, 495–500 (2008).

[11]S. Redner, "Fractal and multifractal scaling of electrical conduction in random resistor networks," preprint arXiv arXiv:0710.1105 (2007).

[12]C. Pennetta, G. Trefan, and L. Reggiani, "Scaling law of resistance fluctuations in stationary random resistor networks," Phys. Rev. Lett. **85**(24), 5238–5241 (2000).

[13]F. M. Willmouth, "Transparency, translucency and gloss," in *Optical Properties of Polymers* edited by G. H. Meeten (Elsevier, 1986), Chap. 5.

[14](a) H. C. Van De Hulst, *Light Scattering by Small Particles* (Dover, 1957); (b) C. Bohren and D. Huffman, *Absorption and Scattering of Light by Small Particles* (Wiley VCH, 1983).

[15](a) M. Kerker, *The Scattering of Light and Other Electromagnetic Radiation* (Academic Press, 1969); (b) M. Quinten, *Optical Properties of Nanoparticle Systems* (Wiley–VCH, 2011).

[16]A. D. Rakic, A. B. Djurisic, J. M. Elazar, and M. Majewski, "Optical properties of metallic films for vertical cavity optoelectronci devices," Appl. Opt. **37**(22), 5271 (1998).

[17]P. Yeh, *Optical Waves in Layered Media* (Wiley, 1988).

[18]A. Heilmann, *Polymer Films with Embedded Metal Nanoparticles* (Springer, 2003), Vol. 52.

[19]B. Johs and J. S. Hale, "Dielectric function representation by B-splines," Phys. Status Solidi A **205**(4), 715–719 (2008).

[20]G. H. Meeten, "Refractive index of colloidal dispersions of spheroidal particles," J. Colloid Interface Sci. **77**(1), 1–5 (1980).

[21](a) A. Killey and G. H. Meeten, "Optical extinction and refraction of concentrated latex dispersions," J. Chem. Soc., Faraday Trans. 2 **77**(4), 587–599 (1981); (b) G. H. Meeten, "An anomalous diffraction theory of linear birefringence and dichroism in colloidal dispersions," J. Colloid Interface Sci. **87**(2), 407–415 (1982); (c) "The intrinsic optical anisotropy of colloidal particles in the anomalous diffraction approximation," *ibid.* **74**(1), 181–185 (1980); (d) "The birefringence of colloidal dispersions in the Rayleigh and anomalous diffraction approximations," *ibid.* **73**(1), 38–44 (1980); (e) *Optical Properties of Polymers* (Elsevier, 1986).

[22](a) R. G. Barrera and A. García-Valenzuela, "Coherent reflectance in a system of random Mie scatterers and its relation to the effective-medium approach," J. Opt. Soc. Am. A **20**(2), 296–311 (2003); (b) R. G. Barrera, A. Reyes-Coronado, and A. García-Valenzuela, "Nonlocal nature of the electrodynamic response of colloidal systems," Phys. Rev. B **75**(18), 184202 (2007); (c) A. García-Valenzuela and R. G. Barrera, "Electromagnetic response of a random half-space of Mie scatterers within the effective-field approximation and the determination of the effective optical coefficients," J. Quant. Spectrosc. Radiat. Transf. **79**, 627–647 (2003).

[23]J. Cserti, "Application of the lattice Green's function for calculating the resistance of an infinite networks of resistors," preprint arXiv cond-mat/9909120 (1999).
[24]D. K. Schroder, *Semiconductor Material and Device Characterization* (IEEE Press & Wiley Interscience, 2006).
[25](a) S. Redner, "Percolation and conduction in a random resistor-diode network," J. Phys. A **14**(9), L349–L354 (1981); (b) S. Redner and A. C. Brown, "Percolation properties of a three-dimensional random resistor-diode network," *ibid.* **14**(8), L285–L290 (1981).
[26]M. Foygel, R. D. Morris, D. Anez, S. French, and V. L. Sobolev, "Theoretical and computational studies of carbon nanotube composites and suspensions: Electrical and thermal conductivity," Phys. Rev. B **71**(10), 104201 (2005).
[27]G. Haacke, "New figure of merit for transparent conductors," J. Appl. Phys. **47**, 4086 (1976).